DO EJECTA FEATURES SUPPORT VOLATILES AS A BASIS FOR CENTRAL PIT CRATERS ON MARS? Paul J. Moretti and Tracy K.P. Gregg, Dept. of Geology, 126 Cooke Hall, University at Buffalo, Buffalo NY 14260 (paulmore@buffalo.buffalo.edu).

Introduction: It has been previously hypothesized that volatiles are present in the target material of some Martian impact craters [1]. Post-impact features such as central pits [1], ejecta ramparts [2,3], curvilinear troughs [4], and pitting [5] represent potential evidence of pre-impact target volatiles released post-impact. These features are commonly observed on Mars, Ganymede, and Callisto [2]; however, their rarity on other planetary bodies suggests a distinct condition essential for their formation.

The existence of impact crater central pits on the Galilean satellites is generally attributed to volatiles present on or near the target surface [6,7,8]. Although the current Martian climate does not support the prolonged presence of liquid surface water [9], the existence of central-pit craters on Mars suggests volatiles (water) below the planet's surface [9].

Here we examine central-pit crater ejecta for dewatering features that could be linked to subsurface target volatiles. If these features are found in the ejecta, their existence would support the presence of volatiles in the target material.

Methodology: Central-pit craters are an existing subset of complex impact craters Utilizing the existing **P**lanetary **I**nteractive **G**.I.S. **W**eb **A**nalyzable **D**atabase (PIGWAD) website [10], a dataset was created including only impact craters containing central pits; this database contained 128 asymmetrical (AS) and 408 symmetrical (SY) craters. The dataset was further constrained to include only craters without visible signs of pit-ring uplift. Using JMARS, each of the 536 central-pit craters were observed in **M**ars **O**rbiting **L**aser **A**ltimeter (MOLA) [11] images, **Th**ermal **Em**ission **I**maging **S**ystem (THEMIS) [12] daytime infrared images, and finally in Mars Reconnaissance Orbiter **C**on**tex**t Camera (CTX) [13] images. Geologic units for each of the remaining eleven craters were identified using Tanaka et al. [14].

A crater centered at: 29.08°S, 98.29°E (Fig. 1) was selected for detailed examination of its ejecta.

Two ejecta features were identified as being consistent with "wet" ejecta: (1) ejecta ramparts (Fig. 2) and (2) curvilinear troughs (Fig. 3). Ejecta ramparts are material appearing as a ridge at or near the margin of the continuous ejecta, where proximal ejecta is topographically higher than the terrain on the distal side of the rampart, but topographically lower than the crest of the rampart, with an asymmetric slope on either side of the rampart crest. Curvilinear troughs are topographic lows between sidewalls in the continuous ejecta blanket exhibiting a curvilinear trend, displaying sidewalls that are parallel to sub-parallel, with closed ends, and trends that are not necessarily radial to the impact crater.

Preliminary Results: An initial examination of this impact crater revealed that: (1) curvilinear troughs are primarily observed in the southern portion of the continuous ejecta blanket (Fig. 3); and (2) many surface features were obscured from view by mantling.

Discussion: The ejecta displays features that may support the presence of sub-surface target volatiles, but the pervasiveness of mantling material on the ejecta locally limits conclusive morphologic interpretations. Although ramparts can be identified at several locations in the continuous ejecta blanket, they are concentrated at the terminus of the continuous ejecta. To date, curvilinear troughs have only been identified in the southeast quadrant of the continuous ejecta. Additional investigation is needed to determine if this spatial distribution is due to crater morphology, obscuration by mantling, weathering, existing terrain, or other conditions.

Additional research is needed to document whether these features exist both inside and outside the constrained dataset. Future research will include examination of additional Martian craters: in the constrained pit crater data subset, pit craters outside the data subset, and craters without central pits.

References: [1] Barlow N.G. and Perez C.B. (2003) *Journal of Geophysical Research*, 108:E8,5085, doi:1029/2001JE002036. [2] Barlow N.G. (1994) *Journal of Geophysical Research*, 99E:5, 927-10,935. [3] Baloga S.M. et al. (2006) *Lunar and Planetary Science XXXVII*, abstract #1309. [4] Tornabene L.L. et al. (2007) *Seventh International Conference on Mars, Abstract* #3288. [5] Tornabene L.L. et al. (2012) *Icarus*, 220, 348-368. [6] Alzate N. and Barlow N.G. (2011) *Icarus*, 211, 1274-1283. [7] Bray V.J. et al. (2012) *Icarus*, 217, 115-129. [8] Elder C.M. et al. (2012) *Icarus*, 221, 831-843. [9] Bramson A.M. et al. (2015) *AGU Geophys. Res. Lett.*, 42, doi: 10.1002/2015GL064844, 6566-6574. [10] Maine A. et al. (2014) *Eighth International Conference on Mars*, Abstract #1044. [10] http://webgis.wr.usgs.gov/pigwad/down/mars_crater_consortium.htm.

[11] Zuber, M.T., et al., The Mars Observer Laser Altimeter Investigation, *J. Geophys. Res.*, *97*, 7781-7797, 1992. [12] P.R. Christensen et al. (2004) *Space Science Reviews*, 110: 85-130. [13] M. C. Malin, et al. (2007), *Journal of Geophysical Research*, 112, E05S04, doi: 10.1029/2006JE002808.

[14] Tanaka, K.L. et al. (2014), USGS Scientific Investigations Map 3292, scale 1:20,000,000, pamphlet 43 p., http://dx.doi.org/ *10.3133/sim3292*.

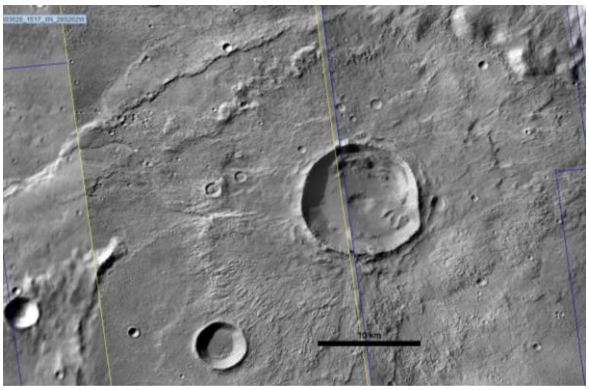

Fig. 1: JMARS CTX rendering composite image of crater ID 244; CTX stamp B02_010390_1500_XI _30S261W, CTX stamp B18__007_964_XN_29S62W over JMARS THEMIS daytime IR v.12.0 image. Scale bar is 10 km.

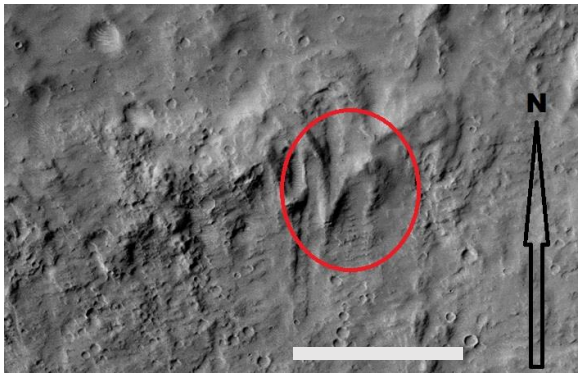

Fig. 2: Portion of *CTX image B02_010390_1500_XI_ 30S261W. Red oval contains examples of ejecta ramparts along the northern terminus of the ejecta blanket. Scale bar is 1 km.*

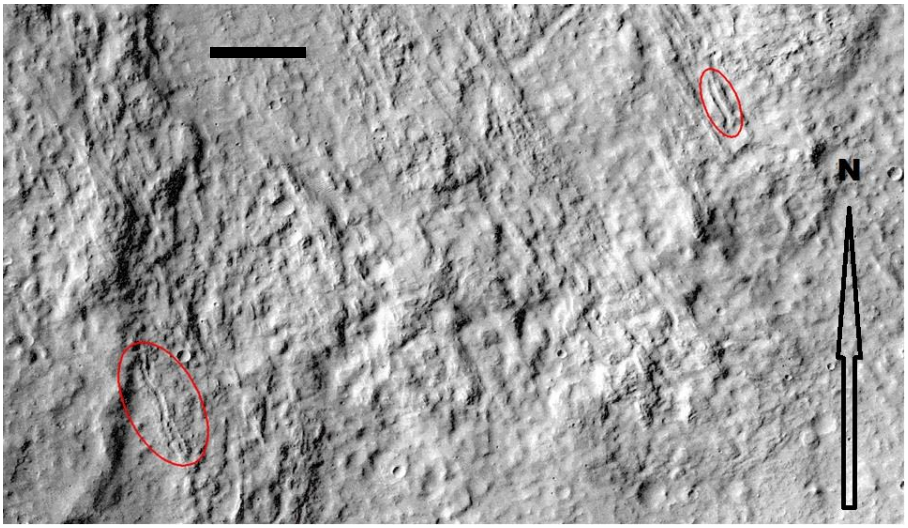

Fig. 3: Portion of *CTX image B02_010390_1500_XI_30S261W. Red ovals contain examples of a curvilinear troughs in the southeast quadrant of the continuous ejecta blanket. Scale bar is 1 km.*